Long-RVOS: A Comprehensive Benchmark for Long-term Referring Video Object Segmentation

Tianming Liang[1], Haichao Jiang[1], Yuting Yang[1], Chaolei Tan[1], Shuai Li[2],
Wei-Shi Zheng[1], Jian-Fang Hu[1*]
[1]Sun Yat-sen University, [2]Shandong University.
liangtm@mail2.sysu.edu.cn, hujf5@mail.sysu.edu.cn
Project Page: https://isee-laboratory.github.io/Long-RVOS

Abstract

*Referring video object segmentation (RVOS) aims to identify, track and segment the objects in a video based on language descriptions, which has received great attention in recent years. However, existing datasets remain focus on short video clips within several seconds, with salient objects visible in most frames. To advance the task towards more practical scenarios, we introduce **Long-RVOS**, a large-scale benchmark for long-term referring video object segmentation. Long-RVOS contains 2,000+ videos of an average duration exceeding 60 seconds, covering a variety of objects that undergo occlusion, disappearance-reappearance and shot changing. The objects are manually annotated with three different types of descriptions to individually evaluate the understanding of static attributes, motion patterns and spatiotemporal relationships. Moreover, unlike previous benchmarks that rely solely on the per-frame spatial evaluation, we introduce two new metrics to assess the temporal and spatiotemporal consistency. We benchmark 7 state-of-the-art methods on Long-RVOS. The results show that current approaches struggle severely with the long-video challenges. To address this, we further propose ReferMo, a promising baseline method that integrates motion information to expand the temporal receptive field, and employs a local-to-global architecture to capture both short-term dynamics and long-term dependencies. Despite simplicity, ReferMo achieves significant improvements over current methods in long-term scenarios. We hope that Long-RVOS and our baseline can drive future RVOS research towards tackling more realistic and long videos.*

1. Introduction

Referring Video Object Segmentation (RVOS) [3, 9, 48] is an emerging task that aims to identify, track and segment the object in the video based on a natural language description. Unlike traditional semi-supervised VOS models that require first-frame masks as the object prompt, RVOS models rely solely on text descriptions to segment the target. Considering its potential applications like video editing, growing efforts have been devoted to this field [9, 17, 27, 32, 35]. Recently, the advent of multi-modal large language models [19, 29, 55] and segment anything models [23, 37] has further accelerated this progress [1, 51, 54, 58].

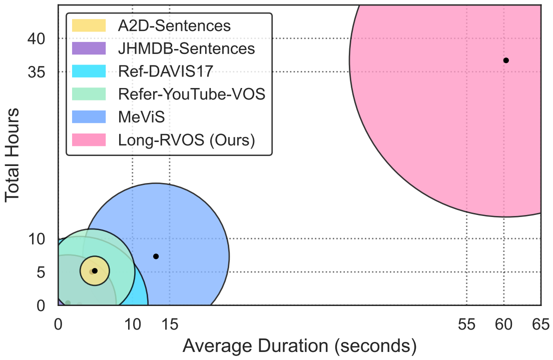

Figure 1. Duration comparison of current RVOS datasets. The circle size indicates the number of frames.

Despite these advances, current RVOS datasets [9, 13, 22, 38] remain limited to short video clips lasting only a few seconds, with target objects clearly visible in most frames. For state-of-the-art (SOTA) methods, in order to capture the target object accurately, it is inevitable to integrate as much spatiotemporal information as possible from the entire video. However, when the video becomes longer, the number of distractors also increases accordingly, making it more challenging to perform sufficient spatiotemporal reasoning and capture the key information. Especially in RVOS, many text descriptions (e.g., “the cat jumping down”) only refer to a brief fragment in the video. In other hand, due to the GPU memory limitation, existing methods [27, 28, 45, 52] typically sample 4∼8 frames per video for training, but use all the frames during inference. As the

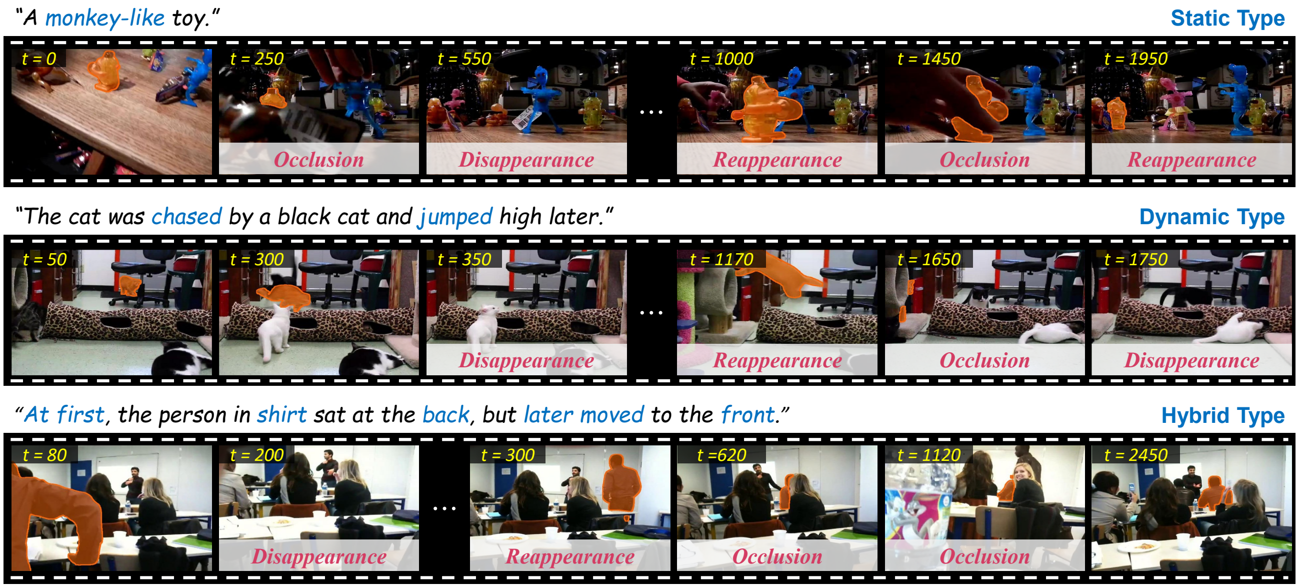

Figure 2. Examples from Long-RVOS dataset, with frame indices displayed in the upper left, and selected objects masked in orange 🟧. Long-RVOS contains extensive long-term videos, where the objects always undergo occlusion, disappearance-reappearance and shot changing. In addition, the objects are annotated with three different types descriptions: *Static*, *Dynamic* and *Hybrid*.

video length increases, the gap between training and inference phases may become more pronounced. Despite these concerns, due to the lack of a long-term RVOS benchmark, the exact challenges posed by longer videos remain unclear.

Another concern lies in the evaluation metrics. Existing RVOS benchmarks [9, 13, 22, 38] typically evaluate performance by simply averaging the frame-wise segmentation metrics (e.g., $\mathcal{J}\&\mathcal{F}$). However, in real-world videos, the target objects do not appear in every frame, due to occlusion and constrained camera views. Therefore, a robust RVOS model should exhibit a sound temporal consistency. This means it should not only segment the target when it is present, but also be able to predict its absence by outputting an empty mask. However, this capability of temporal consistency can not be adequately reflected by existing metrics.

To address these gaps, this work proposes **Long-RVOS**, a large-scale benchmark for long-term video object segmentation. Long-RVOS is the first minute-level dataset in RVOS field, designed to tackle various realistic long-video challenges such as frequent occlusion, disappearance-reappearance and shot changing, as shown in Figure 1 and Figure 2. Additionally, we introduce two new metrics for better evaluation of temporal consistency: tIoU, which measures the temporal overlap between predicted and ground-truth mask sequences; and vIoU, which further measures the spatiotemporal volume overlap between them. We benchmark 7 SOTA methods on Long-RVOS. The results demonstrate that while notable progress has been achieved in existing short-term benchmarks, these SOTA models still significantly struggle in realistic long-term scenarios, in both frame-level segmentation and video-level temporal consistency.

To tackle the challenges posed by Long-RVOS, we present a baseline method **ReferMo**, which integrates additional motion frames to expand the temporal receptive field during training, and employs a local-to-global architecture to perceive both static attributes, short-term dynamics and long-term dependencies. Specifically, ReferMo decomposes each video into a sequence of clips, each consisting of a high-resolution keyframe and multiple low-resolution motion frames. Then, it perceives the static appearance and short-term motion within local video clip, and captures the global target in long-term context via inter-clip interactions. In this way, the temporal receptive field is expanded from multiple frames to multiple clips, but the training cost does not increase significantly. Despite simplicity, ReferMo achieves significant improvements over existing RVOS approaches, serving a promising baseline for long-term referring video object segmentation.

To summarize, our contributions are two folds. **1)** We build Long-RVOS, the first large-scale long-term RVOS benchmark. In Long-RVOS, we provide explicit description types and introduce new metrics to enable more comprehensive evaluation. **2)** We benchmark 7 SOTA approaches on Long-RVOS, and propose a promising baseline ReferMo to address the challenges in long-video scenarios. These contributions establish a foundation for developing more robust RVOS models to handle realistic long videos.

Table 1. Statistical overview of representative RVOS datasets. Long-RVOS features the longest video duration and the most diverse object classes. Besides, Long-RVOS offers explicit text description types for finer-grained evaluation.

Dataset	Year	Videos	Mean duration	Total duration	Mean frames	Masks	Objects	Object classes	Text	Text type
A2D-Sentences [13]	2018	3,782	4.9s	5.2h	3.2	58k	4,825	6	6,656	✗
JHMDB-Sentences [13]	2018	928	1.3s	0.3h	34.3	32k	928	1	928	✗
Ref-DAVIS17 [22]	2018	90	2.9s	0.1h	69.0	14k	205	78	1,544	✗
Refer-YouTube-VOS [38]	2020	**3,978**	4.5s	5.0h	27.2	131k	7,451	94	15,009	✗
MeViS [9]	2023	2,006	13.2s	7.3h	79.0	443k	**8,171**	36	**28,570**	✗
Long-RVOS (ours)	2025	2,193	**60.3s**	**36.7h**	**361.7**	**2.1M**	6,703	**163**	24,689	✓

2. Related Works

RVOS Benchmarks. Given an object description, RVOS aims to identify, tracking and segment the referring object throughout the video. This task was initially introduced by Gavrilyuk et al. [13] and Khoreva et al. [22] in 2018, and has gradually become a popular topic in vision-language understanding. Gavrilyuk et al. [13] built A2D-Sentences and JHMDB-Sentences, which focus on distinguishing different actors in a video through the descriptions about appearance and actions. Khoreva et al. [22] built Ref-DAVIS17 [22], which covers more diverse object types. Later, Ref-Youtube-VOS [38] was developed to further expand the benchmark scale in this field. Recently, MeViS [9] was proposed to highlight the importance of motion understanding in RVOS task. Despite the efforts, these benchmarks remain limited to short video clips lasting only a few seconds, with target objects clearly visible in most frames. Besides, they also lack sufficient evaluation mechanisms to consider the models' specific capabilities in various aspects.

RVOS Approaches. Recent methods are primarily based on Transformer architecture, represented by MTTR [3] and ReferFormer [48]. For a consistent object identification across the frames, follow-up works [16, 17, 32, 41] focus on integrating more object-level temporal information. ReferDINO [27] further improves the visual-language understanding by inheriting the object grounding capability of GroundingDINO [30]. Meanwhile, the recent emergence of segment anything models, i.e., SAM [23] and SAM2 [37], provides unique opportunity for downstream segmentation tasks. Some frontier studies [1, 7, 28, 51] explore to incorporate SAM and SAM2 into RVOS approaches. For example, VideoLISA [1] incorporates large language models with SAM for reasoning video segmentation. SAMWISE [7] integrate text prompts into SAM2 through trainable adapters. While these models achieve great progress in current short-video benchmarks, their abilities and robustness in handling real-world long videos is still unclear.

Long-term Video Understanding. Real-world videos are always long, untrimmed, and involves multiple events. To promote research into long-term video understanding, many large-scale benchmarks [4, 12, 33, 47] have been constructed. However, these benchmarks are mainly constructed for video question answering and temporal action localization, containing only sparse annotations such as timestamps, action labels and captions. To support object-level long-term understanding, some datasets including VidOR [39] and LaSOT [11] also provide dense annotations of bounding boxes. However, long-video datasets with pixel-level dense annotations are still very scarce. Recently, LVOS [18] is built for long-term video object segmentation. However, it is limited in scale and lacks text annotation. In this work, we build Long-RVOS, the first large-scale benchmark for long-term video object segmentation, providing both pixel-wise annotations and diverse object descriptions.

3. Long-RVOS

3.1. Video Collection

Previous RVOS datasets [9, 13, 22, 38] were typically constructed by providing text annotations on their corresponding VOS datasets (e.g., DAVIS17 [36], YouTube-VOS-2019 [50] and MOSE [10]). However, the existing long-term VOS datasets like LVOS [18] are limited in scale (only 720 videos), and most videos feature only one object target. Therefore, in order to establish a large-scale and diverse RVOS benchmark, we bypass the existing VOS datasets and turn to multi-source long video datasets. Specifically, we integrate three long-video datasets: TAO [8], VidOR [39], and Ego-Exo4D [14]. Additionally, TAO is a federated dataset combining multiple sources like Charades [40], LaSOT [11], ArgoVerse [5], AVA [15], YFCC100M [43], BDD-100K [53], and HACS [57]. These datasets typically provide bounding box annotations on sparse frames. Then, we select videos and objects based on the following criteria:

- The video duration exceeds 20 seconds.
- Objects that belong to background, ambiguous or unknown categories are excluded.
- Each selected video must contain more than two valid objects, and at least one object is not continuously visible.

With these criteria, we have initially collected over 3K videos and 8K objects as candidates. After careful inspec-

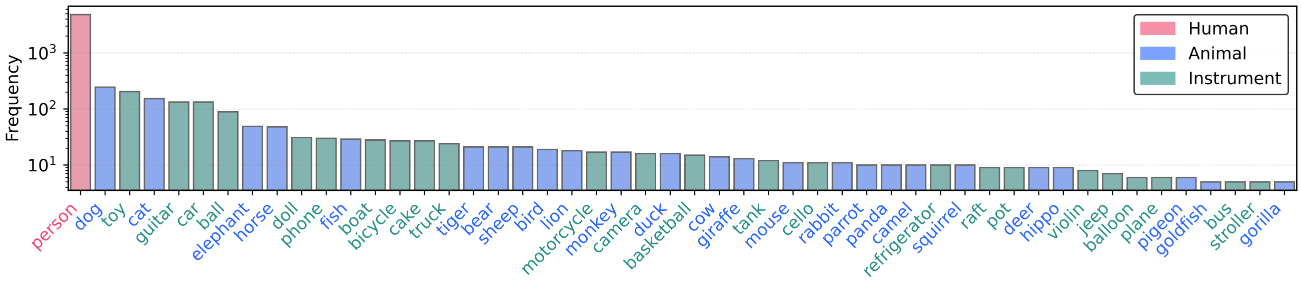

Figure 3. Frequency distribution of the Top-50 object categories.

tions on quality, we finally select 2,193 videos and 6,703 objects to build Long-RVOS.

3.2. Dataset Annotation.

Text Annotation. We develop an online platform for annotating object descriptions. This platform randomly samples a video from our dataset and displays it, with all target objects highlighted by bounding boxes. To ensure the diversity of annotations, each video can be sampled repeatedly at most three times. The annotators consisting of 20 college students are asked to watch the videos and provide the following three types of descriptions for each object:

- **Static type** includes appearance (e.g., colors and shapes), relative position (e.g., “the left cat”), and environmental context (e.g., “on the grass”).
- **Dynamic type** includes motions, changes over time (e.g., in position or state) and interactions with other entities (e.g., “the cat chasing a mouse”).
- **Hybrid type** integrates both static and dynamic attributes to provide comprehensive object cues.

The key annotation principle is that every single description, regardless of type, must clearly distinguish the target object from others. For objects that cannot be distinguished by only static or dynamic attributes, the corresponding type of annotation can be skipped. After this annotation phase, we have collected over 30K text descriptions. These annotations and the corresponding videos are then sent to a validation team formed by three experts for quality verification. Any descriptions that violate our principle are directly removed. Besides, we do not use techniques like synonym replacement to artificially scale up the text annotations, keeping the dataset clear and authentic to support reliable RVOS training. Finally, we gather 24,689 high-quality descriptions for building Long-RVOS.

Mask Annotation. Our source datasets [8, 14, 39] have provided sparse bounding-box annotations. For each object, we segment the video into clips based on the annotated frames. Then, we utilize SAM2 [37], the state-of-the-art VOS model, to track the objects within each clip and produce high-quality masks, by regarding the annotated bounding box as the first-frame prompt. To ensure annotation quality, we conduct an iterative *check–correct* workflow. Specifically, the validation team checks every object's mask separately in the video, and marks the objects with inaccurate annotations. To facilitate the correction process, we develop an interactive annotation tool based on SAM2. This tool loads a marked object each time and visualizes its masks in the video. Nine annotators use our tool to refine the masks with point or box prompts, and remove masks from object-absent frames. The corrected results are then returned to the checking queue, and this *check–correct* loop repeats until all mask annotations are qualified.

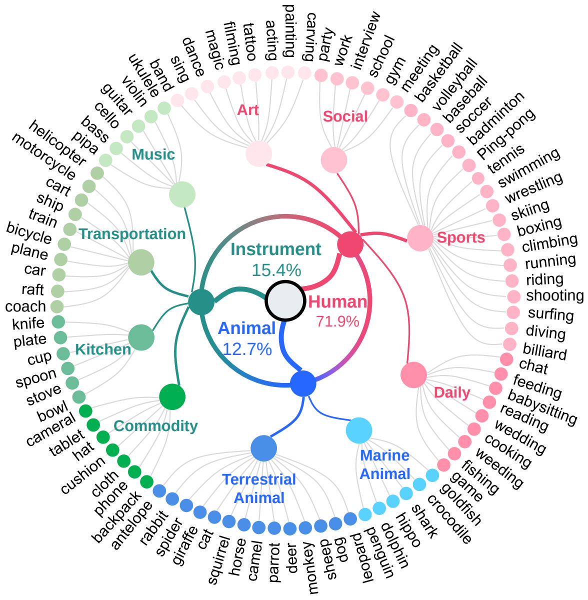

Figure 4. Overview of objects and scenes in Long-RVOS.

3.3. Dataset Statistics

A detailed comparison with five existing RVOS datasets is shown in Table 1. Notably, Long-RVOS offers significantly longer video duration than existing datasets. In addition, it contains the largest number of object classes and mask annotations. The large scale of Long-RVOS supports comprehensive training and evaluation of RVOS models.

Diverse Objects and Scenes. Long-RVOS is constructed by integrating multiple sources of video datasets, achieving a wide variety of objects and scenes, as illustrated in Figures 3 and 4. These sources include indoor videos from Charades [40], outdoor videos from LaSOT [11], movie scenes

Table 2. Distribution of description types.

Type	*Static*	*Dynamic*	*Hybrid*
Percentage	35.03%	32.45%	32.52%

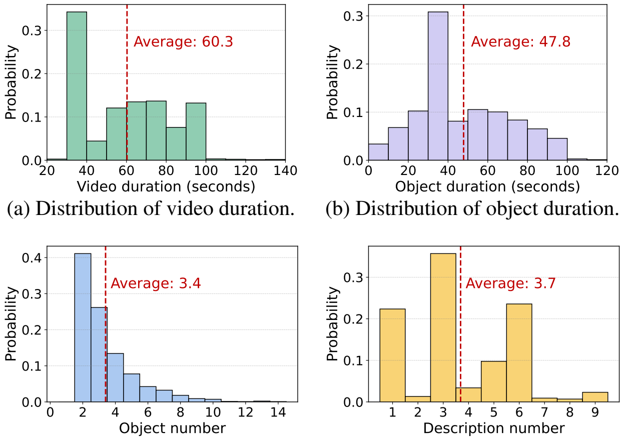

(a) Distribution of video duration.

(b) Distribution of object duration.

(c) Number of objects per video.

(d) Description number per object.

Figure 5. Representative statistics of Long-RVOS.

from AVA [15], egocentric videos from Ego-Exo4D [14], and more diverse videos from other datasets [39, 43, 57]. In total, Long-RVOS contains 163 object categories, significantly surpassing the existing RVOS datasets. While Long-RVOS primarily focuses on human instances (71.9%), it also covers a diverse range of animals (12.7%) and instruments (15.4%). In Figure 5, we present further statistics on the videos and objects in Long-RVOS. Notably, the object number of each video spans from 2 to 14, preventing over-reliance on the most salient object and highlighting text-guided segmentation. Such extensive visual diversity ensures that models are tested against a wide array of complex, real-world scenarios.

Diverse Descriptions. In real-world applications, user queries are always unpredictable. They might refer to salient attributes or instantaneous actions. To enable more comprehensive evaluation of model capabilities, Long-RVOS introduces three distinct types of text descriptions — *Static*, *Dynamic*, and *Hybrid*. By explicitly categorizing these types, Long-RVOS prevents evaluation bias toward specific attribute cues (e.g., colors or positions), ensuring a fair and robust assessment. As shown in Table 2, Long-RVOS maintains a balanced distribution among these three description types. In addition, Figure 5d illustrates that the description number for each object can vary from 1 to 9. These properties encourage comprehensive learning of diverse object attributes. We also present the wordcloud of Long-RVOS is in Figure 6. Together, the diversity in both visual content and textual descriptions establishes Long-RVOS as a truly comprehensive benchmark for the training and evaluation of long-form RVOS models.

Figure 6. Wordcloud of descriptions.

3.4. Evaluation Metrics

Previous RVOS benchmarks tend to evaluate model performance with the frame-wise spatial metrics, such as $\mathcal{J}\&\mathcal{F}$. Here, $\mathcal{J}$ denotes the Intersection-over-Union (IoU) between the predicted and ground-truth masks, $\mathcal{F}$ measures the contour accuracy, and $\mathcal{J}\&\mathcal{F}$ is their average over all the frames. However, these metrics focus solely on the per-frame segmentation quality, neglecting the temporal consistency. A robust RVOS model should accurately segment the target when it is present and correctly output an empty mask when it is absent. Inspired by the field of spatiotemporal video grounding [42, 56], we additionally introduce two new metrics, tIoU and vIoU, in Long-RVOS to individually evaluate the temporal and spatiotemporal performance.

Formally, let $\hat{M}_t, M_t \in \{0,1\}^{H\times W}$ denote the predicted and ground-truth masks at t-th frame, respectively, where $t \in [1, T]$. The frame-index sets of non-empty masks are defined as $\hat{\mathcal{T}} = \{t \mid \|\hat{M}_t\|_0 > 0\}$ (for predictions) and $\mathcal{T} = \{t \mid \|M_t\|_0 > 0\}$ (for the ground-truth), where the ℓ_0-norm $\|\cdot\|_0$ denotes the count of non-zero elements. Then, tIoU is obtained by computing their IoU as follows:

$$\mathrm{tIoU} = \frac{T_i}{T_u}, \quad \text{where } T_i = \hat{\mathcal{T}} \cap \mathcal{T} \text{ and } T_u = \hat{\mathcal{T}} \cup \mathcal{T}, \quad (1)$$

and vIoU computes the volume IoU between predicted and ground-truth mask sequences:

$$\mathrm{vIoU} = \frac{1}{T_u}\sum_{t\in T_i} \mathcal{J}_t, \quad \text{where } \mathcal{J}_t = \frac{\hat{\mathcal{M}}_t \cap \mathcal{M}_t}{\hat{\mathcal{M}}_t \cup \mathcal{M}_t}. \quad (2)$$

By combining the spatial metric $\mathcal{J}\&\mathcal{F}$, temporal metric tIoU and spatiotemporal metric vIoU, Long-RVOS establishes a rigorous evaluation protocol for RVOS research.

4. ReferMo: A Baseline Approach

As illustrated in Figure 7, ReferMo decomposes the video into a sequence of clips, each consisting of a high-resolution keyframe and subsequent low-resolution motion frames. Then, it perceives the static appearance and short-term motion within local video clip, and captures the object target

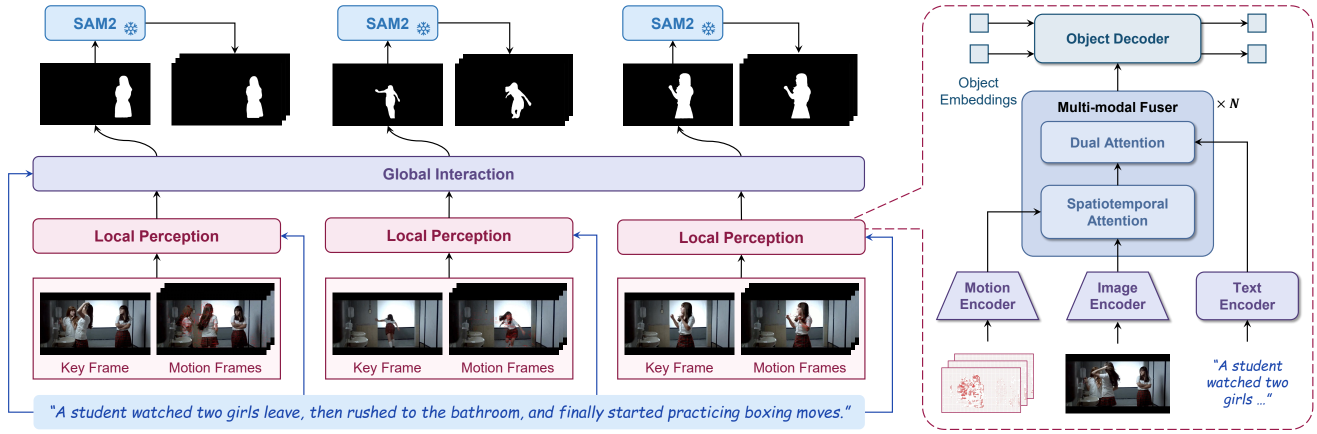

Figure 7. Overview of ReferMo. A video is decomposed into clips (keyframe + motion frames). ReferMo perceives the static attributes and short-term motions within each clip, then aggregates inter-clip information capture the global target. Notably, ReferMo is supervised by only keyframe masks, and SAM2 is only used at inference for target tracking in subsequent frames.

in long-term context by integrating the cross-clip information. Critically, ReferMo only predicts target masks over the keyframes, and the masks on the remain frames are generated by a pretrained mask tracker (e.g., SAM2 [37]). In this way, ReferMo achieves a trade-off between training costs and long-term understanding without processing a large number of high-resolution frames.

4.1. Video Decomposition

Typically, a long-term video is composed of multiple shots, and the video frames within each shot often show significant temporal redundancy. This redundancy can be efficiently described by motion information to reduce the frame-by-frame computations. Inspired by Video-LaVIT [20], we employ the MPEG-4 [25] compression technique to extract keyframe and motion information from the videos. More sophisticated (but expensive) keyframe selection strategies [46, 49] can also be explored, but they are not the primary focus of this work. In MPEG-4, a video is decomposed into multiple clips, where each clip consists of a keyframe $\mathcal{I} \in \mathbb{R}^{H\times W\times 3}$ and the motion vectors $\mathcal{M} \in \mathbb{R}^{T\times \frac{H}{16}\times \frac{W}{16}\times 2}$ of its subsequent T frames. Unlike the dense optical flow, these motion vectors can be directly extracted during the compressed video decoding process, making them well-suited for processing large-scale, long-term videos. More details of motion extraction process are provided in the supplementary.

4.2. From Local Perception to Global Interaction

Different from the previous RVOS methods [27, 32, 52] that perform vision-language fusion on each single frame, we introduce motion representations to enable clip-level vision-language fusion. For each video clip, as shown in the right part of Figure 7, the local perceiver encodes the text, keyframe and motion information through three separate encoders, and then employs a multi-modal fuser to progressively aggregate these information for clip-level object extraction. By collecting the objects across video clips, we perform global temporal interaction to enable consistent object prediction and long-term temporal understanding.

Motion Encoder. The motion vectors are first embeded into a d-dimensional space via a linear projector. Then, the motion encoder performs self-attention separately along the spatial and temporal dimensions to extract the spatiotemporal motion features $M \in \mathbb{R}^{T\times \frac{H}{16}\times \frac{W}{16}\times d}$. Notably, we implement the spatial attention as deformable attention due to the large number of spatial tokens.

Image-Motion Fusion. Modern image encoders (e.g., Swin Transformer [31]) typically output multi-scale feature maps $I_i \in \mathbb{R}^{H_i\times W_i\times d}$, $i \in [1, 4]$. To match these spatial resolutions, we adopt a series of spatial convolutions with specific strides over the motion features M to produce multi-scale motion features $M_i \in \mathbb{R}^{T\times H_i\times W_i\times d}$. At each scale i, we treat the keyframe feature I_i as *query* and perform cross-attention along the temporal dimension to aggregate M_i into $\widetilde{M}_i \in \mathbb{R}^{H_i\times W_i\times d}$. To avoid undesired motion noise, we fuse the keyframe and motion features via the spatial-aware and channel-aware gating mechanisms:

$$M_i^* = (\underbrace{\sigma(I_i \cdot W_{down}^I)}_{\text{Spatial Gate}} \odot (\widetilde{M}_i \cdot W_{down}^M)) \cdot W_{up}, \tag{3}$$

$$F_i = I_i + \underbrace{\gamma_i}_{\text{Channel Gate}} \odot \max(M_i^*, 0)^2, \tag{4}$$

where $W_{down}^I, W_{down}^M \in \mathbb{R}^{d\times r}$ indicate the low-rank projectors that compress the features to a lower dimension r, and $W_{up} \in \mathbb{R}^{r\times d}$ resorts the dimension. σ denotes Sigmoid function and $\odot$ denotes Hadamard product. $\gamma \in \mathbb{R}^d$ is a learnable vector to modulate the channel-wise weights.

Vision-Language Fusion. We use dual cross-attention [26, 30] for deep vision-language fusion. Formally, given the

Table 3. Comparison on Long-RVOS test set. FPS is estimated at 360P on Nvidia A6000 GPUs, excluding the video loading time.

Method	Static			Dynamic			Hybrid			Overall			FPS
	$\mathcal{J}\&\mathcal{F}$	tIoU	vIoU	$\mathcal{J}\&\mathcal{F}$	tIoU	vIoU	$\mathcal{J}\&\mathcal{F}$	tIoU	vIoU	$\mathcal{J}\&\mathcal{F}$	tIoU	vIoU	
Without SAM / SAM2													
SOC [32] NeurIPS'23	39.3	71.8	33.9	38.8	73.2	34.2	37.7	71.9	32.5	38.6	72.3	33.5	53.8
MUTR [52] AAAI'24	42.8	72.6	38.7	41.2	73.5	37.7	42.4	72.3	38.1	42.2	72.8	38.2	20.4
ReferDINO [27] ICCV'25	50.9	73.6	46.0	45.4	73.8	41.5	48.7	**73.1**	44.0	48.4	73.5	43.9	46.4
With SAM / SAM2													
VideoLISA [1] NeurIPS'24	17.7	65.8	14.0	12.7	71.4	5.3	11.5	70.0	4.6	14.0	69.0	8.1	6.6
GLUS [28] CVPR'25	25.2	61.8	21.6	27.2	62.7	23.9	24.8	60.3	20.6	25.7	61.6	22.0	3.6
SAMWISE [7] CVPR'25	41.3	65.5	31.3	40.4	67.6	31.3	41.0	66.9	30.8	40.9	66.6	31.1	7.0
RGA3 [45] ICCV'25	22.1	59.8	16.9	23.4	61.0	19.0	22.2	59.2	16.7	22.5	60.0	17.5	8.7
ReferMo (Ours)	**55.8**	**73.6**	**47.5**	**49.3**	**74.2**	**42.4**	**53.3**	72.9	**45.4**	**52.9**	**73.6**	**45.2**	52.5

clip-level vision features $F \in \mathbb{R}^{N\times d}$ and the language features $E \in \mathbb{R}^{L\times d}$, where N and L individually denote their token number, we derive the cross-modal enhanced vision features $\widetilde{F}$ and language features $\widetilde{E}$ as follows:

$$\begin{cases} \widetilde{F} = \mathrm{Softmax}(\mathcal{A}) \cdot E, \\ \widetilde{E} = \mathrm{Softmax}(\mathcal{A}^\top) \cdot F, \end{cases} \quad \text{where } \mathcal{A} = \frac{FE^\top}{\sqrt{d}}. \tag{5}$$

For simplicity, the linear projections for multi-head attentions are omitted. The output features $\widetilde{F}$ and $\widetilde{E}$ are then fed into the object decoder to extract object features.

Global Interaction. To enable consistent object prediction and long-term temporal understanding, we collect the object features across video clips to perform global temporal interactions. Following ReferDINO [27], we use the Hungarian algorithm [24] to align the objects clip-by-clip. Then, we perform temporal self-attention over the aligned object features to achieve global modeling. For better modality alignment, we also infuse the language information $\widetilde{E}$ into the object features through a cross-attention layer. Finally, the interacted object features are sent to the segmentation head for generating instance masks. Note that these masks are only predicted for the key frame within each clip, serving as object anchors for SAM2's mask propagation in subsequent frames. More details are present in the supplementary.

5. Experiments

5.1. Experiment Setup

Dataset Split. Long-RVOS is a large-scale dataset containing 2,193 videos and 24,689 descriptions. It is split into three subsets: a training set of 1,855 videos and 20,722 descriptions, a validation set of 112 videos and 1,326 descriptions, and a test set of 226 videos and 2,641 descriptions.

Evaluation Metrics. We use three kinds of evaluation metrics: the spatial metric $\mathcal{J}\&\mathcal{F}$, the temporal metric tIoU and the spatiotemporal metric vIoU. Long-RVOS provides three types of descriptions: *Static*, *Temporal* and *Hybrid*. We report performance for each type separately and overall. We also recommend reporting FPS because efficiency is a major concern for long-video processing.

Implementation Details. We follow the default hyperparameter settings of ReferDINO [27] and use Swin-Tiny as the backbone. For SAM2 [37], we use the $\mathrm{sam2.1\_hiera\_large}$ version. In MPEG-4 [25], each video clip typically consists of a keyframe and the motion vectors for up to 11 subsequent frames. During training, we randomly sample 6 clips and use 3-frame motion vectors. The input frames are resized to have the longest side of 640 pixels and the shortest side of 360 pixels during both training and evaluation. Following MeViS [9], we do not use image segmentation datasets (e.g., RefCOCO/+/g [21, 34]) for pretraining. We train ReferMo on Long-RVOS dataset for 6 epochs, which take 24 hours on 8 Nvidia A6000 GPUs.

5.2. Benchmark Results

Overall Comparison. We compare ReferMo with 7 recent RVOS methods on Long-RVOS. For a fair comparison, all the models are trained solely on Long-RVOS, with no external segmentation datasets used. As demonstrated in Table 3, realistic long-video scenarios remain a significant challenge for current RVOS models. While the SAM2-based methods [7, 28, 45] achieve SOTA performance on existing short-term benchmarks, they significantly struggle in Long-RVOS. This suggests that their improvements may primarily stem from SAM2's superior tracking and segmentation capabilities, rather than better language-object understanding. As videos grow longer and more complex, it becomes more challenging to maintain accurate video-language reasoning and consistently distinguish the objects, which leads to their performance degradation. This issue is more pronounced for those MLLM-based approaches [1, 28, 45], which typically require massive multi-source training data to bridge the gap between reasoning and segmentation. In contrast, our ReferMo demonstrates remarkable data efficiency and inference speed, while achieving significant improvements in long-video understanding.

Fine-grained Evaluation. For most models, the highest performance is achieved on the Static type, followed by Hybrid, and the lowest on Dynamic. This implies a strong bias in current RVOS models toward static attributes, as well as

Table 4. Oracle analysis and ablation studies.

(a) Oracle analysis with SAM2.

Dataset		Point	Box	Mask
MeViS [9]	Valid_u	77.3	80.0	80.6
Long-RVOS	Valid	54.4	55.9	56.6
	Test	54.3	55.6	55.6

(b) Effect of the video decomposition.

Strategy	$\mathcal{J}$	$\mathcal{F}$	$\mathcal{J}\&\mathcal{F}$
Baseline [27]	48.1	49.7	48.9
+ keyframe.	49.5	50.6	50.0
+ keyframe & motion	**50.3**	**51.8**	**51.1**

(c) Different mask propagation methods.

Method	$\mathcal{J}$	$\mathcal{F}$	$\mathcal{J}\&\mathcal{F}$
Xmem++ [2]	49.9	51.0	50.4
Cutie [6]	49.6	50.9	50.2
SAM2 [37]	**52.2**	**53.5**	**52.9**

Table 5. Keyframe performance with global interaction.

Global	Motion	$\mathcal{J}$	$\mathcal{F}$	$\mathcal{J}\&\mathcal{F}$
		49.8	50.4	49.8
✓		49.5	50.6	50.0
	✓	50.0	51.4	50.7
✓	✓	50.3	51.8	51.1

significant challenges in dynamic and temporal understanding. Furthermore, while $\mathcal{J}\&\mathcal{F}$ scores vary significantly, tIoU is relatively stable across methods and types. This indicates that high $\mathcal{J}\&\mathcal{F}$ scores do not necessarily correlate with strong temporal consistency, and the introduction of tIoU effectively disentangles these aspects. Additionally, the consistently low vIoU scores across all models suggest that previous evaluations relying solely on frame-averaging metrics may have overestimated the practical robustness of RVOS models. Against this challenging backdrop, our ReferMo showcases consistent performance improvements over SOTA competitors across all types and metrics.

Oracle Analysis. We provide SAM2 with first-frame ground-truth object prompts (i.e., points, boxes or masks) and evaluate its tracking performance. As shown in Table 4a, the oracle results for Long-RVOS (54.3∼56.6 $\mathcal{J}\&\mathcal{F}$) are significantly lower than those for MeViS (77.3∼80.6 $\mathcal{J}\&\mathcal{F}$). The notable performance gap of nearly 25% demonstrates the long-term challenges in Long-RVOS.

5.3. Ablation Studies

Effect of Video Decomposition. In contrast to prior RVOS models [27, 32, 52] that directly performs temporal reasoning on the entire video, our ReferMo decomposes the video into clips (keyframe + motion information) to enable local-to-global reasoning. To explore the effect of our strategy, we report performance on the keyframes (before SAM2 tracking) in Table 4b. The results show that the keyframe-based decomposition strategy surpasses the baseline by 1.1 $\mathcal{J}\&\mathcal{F}$. Further incorporating motion information yields an additional +1.1 $\mathcal{J}\&\mathcal{F}$ gain. Moreover, unlike the baseline, our ReferMo is only trained with keyframe ground truths, yet it achieves much better performance in long-video scenarios. These results encourage further exploration of sparse-frame supervision for RVOS task.

Effect of Different Mask Propagation Strategies. We replace SAM2 with other propagation models (e.g., Xmem++ [2] and Cuite [6]) in Table 4c, which shows that SAM2 contributes 2.5∼2.7 $\mathcal{J}\&\mathcal{F}$ gains to overall performance. Notably, by cross-referencing Table 3 and Table 4c, we observe that even combining with these traditional propagation models, our ReferMo still outperforms existing SAM2-based RVOS methods. These results validate the robustness of our approach.

Table 6. Overall $\mathcal{J}\&\mathcal{F}$ results at various object occlusion rates.

Method	[0, 0.25]	[0.25, 0.5)	[0.5, 0.75)	[0.75, 1]
RGA3 [45]	25.6	17.8	19.1	10.4
MUTR [52]	47.4	38.5	30.8	17.4
ReferDINO [27]	53.3	45.0	36.7	25.6
SAMWISE [7]	39.9	39.3	38.8	38.0
ReferMo (Ours)	**54.6**	**50.6**	**46.5**	**39.7**

Effects of Global Interaction and Motion Information. In Table 5, we explore the effect of global interaction. We observe that a naive local-to-global structure only yields a marginal gain of +0.2 $\mathcal{J}\&\mathcal{F}$ (Row 2 *vs.* Row 1). This is because the sparse keyframes provide insufficient context for global reasoning. In contrast, when we integrate motion features to expand the local window, performance increases significantly by 1.1 $\mathcal{J}\&\mathcal{F}$ (Row 4 *vs.* Row 2).

Robustness of Keyframe Methods. As a keyframe-based approach, ReferMo may encounter challenges when target objects are absent from selected keyframes. To evaluate its robustness, we present the results under varying object occlusion rates in Table 6. The results show that ReferMo consistently outperforms all competitors across all occlusion brackets. Moreover, as the occlusion rate increases, ReferMo maintains a consistent performance advantage over most methods. Although its leading margin over SAMWISE [7], which uses a streaming post-correction mechanism, narrows at high-occlusion scenarios, ReferMo's overall performance is significantly superior. Therefore, despite relying soly on keyframe reasoning, ReferMo remains sufficiently robust in most non-extreme cases.

6. Conclusion

In this work, we introduce Long-RVOS, a large-scale benchmark for long-term referring video object segmentation, comprising over 2,000 videos averaging 60+ seconds to address the limitations of existing short-term datasets. To enable comprehensive and rigorous evaluation, we provide three types of descriptions and two novel metrics, tIoU and vIoU. Results on Long-RVOS indicate that current RVOS methods struggle severely in long-video scenarios. Furthermore, we propose ReferMo, a simple motion-enhanced baseline that significantly outperforms existing SOTA methods on long-term videos. We believe that Long-RVOS and ReferMo will provide a foundation for future research to develop robust models tackling real-world long videos.

References

[1] Zechen Bai, Tong He, Haiyang Mei, Pichao Wang, Ziteng Gao, Joya Chen, Zheng Zhang, and Mike Zheng Shou. One token to seg them all: Language instructed reasoning segmentation in videos. *Advances in Neural Information Processing Systems*, 37:6833–6859, 2024. 1, 3, 7, 2

[2] Maksym Bekuzarov, Ariana Bermudez, Joon-Young Lee, and Hao Li. Xmem++: Production-level video segmentation from few annotated frames. In *Proceedings of the IEEE/CVF International Conference on Computer Vision*, pages 635–644, 2023. 8

[3] Adam Botach, Evgenii Zheltonozhskii, and Chaim Baskin. End-to-end referring video object segmentation with multimodal transformers. In *Proceedings of the IEEE/CVF Conference on Computer Vision and Pattern Recognition*, pages 4985–4995, 2022. 1, 3

[4] Fabian Caba Heilbron, Victor Escorcia, Bernard Ghanem, and Juan Carlos Niebles. Activitynet: A large-scale video benchmark for human activity understanding. In *Proceedings of the ieee conference on computer vision and pattern recognition*, pages 961–970, 2015. 3

[5] Ming-Fang Chang, John Lambert, Patsorn Sangkloy, Jagjeet Singh, Slawomir Bak, Andrew Hartnett, De Wang, Peter Carr, Simon Lucey, Deva Ramanan, et al. Argoverse: 3d tracking and forecasting with rich maps. In *Proceedings of the IEEE/CVF Conference on Computer Vision and Pattern Recognition*, pages 8748–8757, 2019. 3

[6] Ho Kei Cheng, Seoung Wug Oh, Brian Price, Joon-Young Lee, and Alexander Schwing. Putting the object back into video object segmentation. In *Proceedings of the IEEE/CVF Conference on Computer Vision and Pattern Recognition*, pages 3151–3161, 2024. 8

[7] Claudia Cuttano, Gabriele Trivigno, Gabriele Rosi, Carlo Masone, and Giuseppe Averta. Samwise: Infusing wisdom in sam2 for text-driven video segmentation. In *Proceedings of the IEEE/CVF Conference on Computer Vision and Pattern Recognition*, 2025. 3, 7, 8, 2

[8] Achal Dave, Tarasha Khurana, Pavel Tokmakov, Cordelia Schmid, and Deva Ramanan. Tao: A large-scale benchmark for tracking any object. In *Computer Vision–ECCV 2020: 16th European Conference, Glasgow, UK, August 23–28, 2020, Proceedings, Part V 16*, pages 436–454. Springer, 2020. 3, 4

[9] Henghui Ding, Chang Liu, Shuting He, Xudong Jiang, and Chen Change Loy. Mevis: A large-scale benchmark for video segmentation with motion expressions. In *Proceedings of the IEEE/CVF International Conference on Computer Vision*, pages 2694–2703, 2023. 1, 2, 3, 7, 8

[10] Henghui Ding, Chang Liu, Shuting He, Xudong Jiang, Philip HS Torr, and Song Bai. Mose: A new dataset for video object segmentation in complex scenes. In *Proceedings of the IEEE/CVF international conference on computer vision*, pages 20224–20234, 2023. 3

[11] Heng Fan, Liting Lin, Fan Yang, Peng Chu, Ge Deng, Sijia Yu, Hexin Bai, Yong Xu, Chunyuan Liao, and Haibin Ling. Lasot: A high-quality benchmark for large-scale single object tracking. In *Proceedings of the IEEE/CVF conference on computer vision and pattern recognition*, pages 5374–5383, 2019. 3, 4

[12] Chaoyou Fu, Yuhan Dai, Yongdong Luo, Lei Li, Shuhuai Ren, Renrui Zhang, Zihan Wang, Chenyu Zhou, Yunhang Shen, Mengdan Zhang, et al. Video-mme: The first-ever comprehensive evaluation benchmark of multi-modal llms in video analysis. *arXiv preprint arXiv:2405.21075*, 2024. 3

[13] Kirill Gavrilyuk, Amir Ghodrati, Zhenyang Li, and Cees GM Snoek. Actor and action video segmentation from a sentence. In *Proceedings of the IEEE conference on computer vision and pattern recognition*, pages 5958–5966, 2018. 1, 2, 3

[14] Kristen Grauman, Andrew Westbury, Lorenzo Torresani, Kris Kitani, Jitendra Malik, Triantafyllos Afouras, Kumar Ashutosh, Vijay Baiyya, Siddhant Bansal, Bikram Boote, et al. Ego-exo4d: Understanding skilled human activity from first-and third-person perspectives. In *Proceedings of the IEEE/CVF Conference on Computer Vision and Pattern Recognition*, pages 19383–19400, 2024. 3, 4, 5

[15] Chunhui Gu, Chen Sun, David A Ross, Carl Vondrick, Caroline Pantofaru, Yeqing Li, Sudheendra Vijayanarasimhan, George Toderici, Susanna Ricco, Rahul Sukthankar, et al. Ava: A video dataset of spatio-temporally localized atomic visual actions. In *Proceedings of the IEEE Conference on Computer Vision and Pattern Recognition*, pages 6047–6056, 2018. 3, 5

[16] Mingfei Han, Yali Wang, Zhihui Li, Lina Yao, Xiaojun Chang, and Yu Qiao. Html: Hybrid temporal-scale multimodal learning framework for referring video object segmentation. In *Proceedings of the IEEE/CVF International Conference on Computer Vision*, pages 13414–13423, 2023. 3

[17] Shuting He and Henghui Ding. Decoupling static and hierarchical motion perception for referring video segmentation. In *Proceedings of the IEEE/CVF Conference on Computer Vision and Pattern Recognition*, pages 13332–13341, 2024. 1, 3

[18] Lingyi Hong, Wenchao Chen, Zhongying Liu, Wei Zhang, Pinxue Guo, Zhaoyu Chen, and Wenqiang Zhang. Lvos: A benchmark for long-term video object segmentation. In *Proceedings of the IEEE/CVF International Conference on Computer Vision*, pages 13480–13492, 2023. 3

[19] Peng Jin, Ryuichi Takanobu, Wancai Zhang, Xiaochun Cao, and Li Yuan. Chat-univi: Unified visual representation empowers large language models with image and video understanding. In *Proceedings of the IEEE/CVF Conference on Computer Vision and Pattern Recognition*, pages 13700–13710, 2024. 1

[20] Yang Jin, Zhicheng Sun, Kun Xu, Liwei Chen, Hao Jiang, Quzhe Huang, Chengru Song, Yuliang Liu, Di Zhang, Yang

Song, et al. Video-lavit: Unified video-language pre-training with decoupled visual-motional tokenization. *arXiv preprint arXiv:2402.03161*, 2024. 6, 1

[21] Sahar Kazemzadeh, Vicente Ordonez, Mark Matten, and Tamara Berg. Referitgame: Referring to objects in photographs of natural scenes. In *Proceedings of the 2014 conference on empirical methods in natural language processing (EMNLP)*, pages 787–798, 2014. 7

[22] Anna Khoreva, Anna Rohrbach, and Bernt Schiele. Video object segmentation with language referring expressions. In *Computer Vision–ACCV 2018: 14th Asian Conference on Computer Vision, Perth, Australia, December 2–6, 2018, Revised Selected Papers, Part IV 14*, pages 123–141. Springer, 2019. 1, 2, 3

[23] Alexander Kirillov, Eric Mintun, Nikhila Ravi, Hanzi Mao, Chloe Rolland, Laura Gustafson, Tete Xiao, Spencer Whitehead, Alexander C Berg, Wan-Yen Lo, et al. Segment anything. In *Proceedings of the IEEE/CVF International Conference on Computer Vision*, pages 4015–4026, 2023. 1, 3

[24] Harold W Kuhn. The hungarian method for the assignment problem. *Naval research logistics quarterly*, 2(1-2):83–97, 1955. 7, 1

[25] Didier Le Gall. Mpeg: A video compression standard for multimedia applications. *Communications of the ACM*, 34 (4):46–58, 1991. 6, 7

[26] Liunian Harold Li, Pengchuan Zhang, Haotian Zhang, Jianwei Yang, Chunyuan Li, Yiwu Zhong, Lijuan Wang, Lu Yuan, Lei Zhang, Jenq-Neng Hwang, et al. Grounded language-image pre-training. In *Proceedings of the IEEE/CVF Conference on Computer Vision and Pattern Recognition*, pages 10965–10975, 2022. 6

[27] Tianming Liang, Kun-Yu Lin, Chaolei Tan, Jianguo Zhang, Wei-Shi Zheng, and Jian-Fang Hu. Referdino: Referring video object segmentation with visual grounding foundations. In *Proceedings of the IEEE/CVF International Conference on Computer Vision*, pages 20009–20019, 2025. 1, 3, 6, 7, 8, 2

[28] Lang Lin, Xueyang Yu, Ziqi Pang, and Yu-Xiong Wang. Glus: Global-local reasoning unified into a single large language model for video segmentation. In *Proceedings of the IEEE/CVF Conference on Computer Vision and Pattern Recognition*, 2025. 1, 3, 7, 2

[29] Haotian Liu, Chunyuan Li, Qingyang Wu, and Yong Jae Lee. Visual instruction tuning. *Advances in neural information processing systems*, 36:34892–34916, 2023. 1

[30] Shilong Liu, Zhaoyang Zeng, Tianhe Ren, Feng Li, Hao Zhang, Jie Yang, Chunyuan Li, Jianwei Yang, Hang Su, Jun Zhu, et al. Grounding dino: Marrying dino with grounded pre-training for open-set object detection. In *European Conference on Computer Vision*, 2024. 3, 6

[31] Ze Liu, Yutong Lin, Yue Cao, Han Hu, Yixuan Wei, Zheng Zhang, Stephen Lin, and Baining Guo. Swin transformer: Hierarchical vision transformer using shifted windows. In *Proceedings of the IEEE/CVF international conference on computer vision*, pages 10012–10022, 2021. 6

[32] Zhuoyan Luo, Yicheng Xiao, Yong Liu, Shuyan Li, Yitong Wang, Yansong Tang, Xiu Li, and Yujiu Yang. Soc: semantic-assisted object cluster for referring video object segmentation. In *Proceedings of the 37th International Conference on Neural Information Processing Systems*, pages 26425–26437, 2023. 1, 3, 6, 7, 8, 2

[33] Karttikeya Mangalam, Raiymbek Akshulakov, and Jitendra Malik. Egoschema: A diagnostic benchmark for very long-form video language understanding. *Advances in Neural Information Processing Systems*, 36:46212–46244, 2023. 3

[34] Junhua Mao, Jonathan Huang, Alexander Toshev, Oana Camburu, Alan L Yuille, and Kevin Murphy. Generation and comprehension of unambiguous object descriptions. In *Proceedings of the IEEE conference on computer vision and pattern recognition*, pages 11–20, 2016. 7

[35] Bo Miao, Mohammed Bennamoun, Yongsheng Gao, and Ajmal Mian. Spectrum-guided multi-granularity referring video object segmentation. In *Proceedings of the IEEE/CVF International Conference on Computer Vision*, pages 920–930, 2023. 1

[36] Jordi Pont-Tuset, Federico Perazzi, Sergi Caelles, Pablo Arbeláez, Alex Sorkine-Hornung, and Luc Van Gool. The 2017 davis challenge on video object segmentation. *arXiv preprint arXiv:1704.00675*, 2017. 3

[37] Nikhila Ravi, Valentin Gabeur, Yuan-Ting Hu, Ronghang Hu, Chaitanya Ryali, Tengyu Ma, Haitham Khedr, Roman Rädle, Chloe Rolland, Laura Gustafson, Eric Mintun, Junting Pan, Kalyan Vasudev Alwala, Nicolas Carion, Chao-Yuan Wu, Ross Girshick, Piotr Dollár, and Christoph Feichtenhofer. Sam 2: Segment anything in images and videos. *arXiv preprint arXiv:2408.00714*, 2024. 1, 3, 4, 6, 7, 8, 2

[38] Seonguk Seo, Joon-Young Lee, and Bohyung Han. Urvos: Unified referring video object segmentation network with a large-scale benchmark. In *Computer Vision–ECCV 2020: 16th European Conference, Glasgow, UK, August 23–28, 2020, Proceedings, Part XV 16*, pages 208–223. Springer, 2020. 1, 2, 3

[39] Xindi Shang, Donglin Di, Junbin Xiao, Yu Cao, Xun Yang, and Tat-Seng Chua. Annotating objects and relations in user-generated videos. In *Proceedings of the 2019 on International Conference on Multimedia Retrieval*, pages 279–287. ACM, 2019. 3, 4, 5

[40] Gunnar A Sigurdsson, Gül Varol, Xiaolong Wang, Ali Farhadi, Ivan Laptev, and Abhinav Gupta. Hollywood in homes: Crowdsourcing data collection for activity understanding. In *Computer Vision–ECCV 2016: 14th European Conference, Amsterdam, The Netherlands, October 11–14, 2016, Proceedings, Part I 14*, pages 510–526. Springer, 2016. 3, 4

[41] Jiajin Tang, Ge Zheng, and Sibei Yang. Temporal collection and distribution for referring video object segmentation. In *Proceedings of the IEEE/CVF International Conference on Computer Vision*, pages 15466–15476, 2023. 3

[42] Zongheng Tang, Yue Liao, Si Liu, Guanbin Li, Xiaojie Jin, Hongxu Jiang, Qian Yu, and Dong Xu. Human-centric spatio-temporal video grounding with visual transformers. *IEEE Transactions on Circuits and Systems for Video Technology*, 32(12):8238–8249, 2021. 5

[43] Bart Thomee, David A Shamma, Gerald Friedland, Benjamin Elizalde, Karl Ni, Douglas Poland, Damian Borth, and

Li-Jia Li. Yfcc100m: The new data in multimedia research. *Communications of the ACM*, 59(2):64–73, 2016. 3, 5

[44] Zhi Tian, Chunhua Shen, and Hao Chen. Conditional convolutions for instance segmentation. In *Computer Vision–ECCV 2020: 16th European Conference, Glasgow, UK, August 23–28, 2020, Proceedings, Part I 16*, pages 282–298. Springer, 2020. 2

[45] Haochen Wang, Qirui Chen, Cilin Yan, Jiayin Cai, Xiaolong Jiang, Yao Hu, Weidi Xie, and Stratis Gavves. Object-centric video question answering with visual grounding and referring. In *Proceedings of the IEEE/CVF International Conference on Computer Vision*, pages 22274–22284, 2025. 1, 7, 8, 2

[46] Xiaohan Wang, Yuhui Zhang, Orr Zohar, and Serena Yeung-Levy. Videoagent: Long-form video understanding with large language model as agent. In *European Conference on Computer Vision*, pages 58–76. Springer, 2024. 6

[47] Chao-Yuan Wu and Philipp Krahenbuhl. Towards long-form video understanding. In *Proceedings of the IEEE/CVF Conference on Computer Vision and Pattern Recognition*, pages 1884–1894, 2021. 3

[48] Jiannan Wu, Yi Jiang, Peize Sun, Zehuan Yuan, and Ping Luo. Language as queries for referring video object segmentation. In *Proceedings of the IEEE/CVF Conference on Computer Vision and Pattern Recognition*, pages 4974–4984, 2022. 1, 3

[49] Zuxuan Wu, Caiming Xiong, Chih-Yao Ma, Richard Socher, and Larry S Davis. Adaframe: Adaptive frame selection for fast video recognition. In *Proceedings of the IEEE/CVF Conference on Computer Vision and Pattern Recognition*, pages 1278–1287, 2019. 6

[50] Ning Xu, Linjie Yang, Yuchen Fan, Dingcheng Yue, Yuchen Liang, Jianchao Yang, and Thomas Huang. Youtube-vos: A large-scale video object segmentation benchmark. *arXiv preprint arXiv:1809.03327*, 2018. 3

[51] Cilin Yan, Haochen Wang, Shilin Yan, Xiaolong Jiang, Yao Hu, Guoliang Kang, Weidi Xie, and Efstratios Gavves. Visa: Reasoning video object segmentation via large language models. *arXiv preprint arXiv:2407.11325*, 2024. 1, 3

[52] Shilin Yan, Renrui Zhang, Ziyu Guo, Wenchao Chen, Wei Zhang, Hongyang Li, Yu Qiao, Hao Dong, Zhongjiang He, and Peng Gao. Referred by multi-modality: A unified temporal transformer for video object segmentation. In *Proceedings of the AAAI Conference on Artificial Intelligence*, pages 6449–6457, 2024. 1, 6, 7, 8, 2, 3

[53] Fisher Yu, Haofeng Chen, Xin Wang, Wenqi Xian, Yingying Chen, Fangchen Liu, Vashisht Madhavan, and Trevor Darrell. Bdd100k: A diverse driving dataset for heterogeneous multitask learning. *Proceedings of the IEEE/CVF Conference on Computer Vision and Pattern Recognition*, pages 2636–2645, 2020. 3

[54] Haobo Yuan, Xiangtai Li, Tao Zhang, Zilong Huang, Shilin Xu, Shunping Ji, Yunhai Tong, Lu Qi, Jiashi Feng, and Ming-Hsuan Yang. Sa2va: Marrying sam2 with llava for dense grounded understanding of images and videos. *arXiv*, 2025. 1

[55] Hang Zhang, Xin Li, and Lidong Bing. Video-llama: An instruction-tuned audio-visual language model for video understanding. In *Proceedings of the 2023 Conference on Empirical Methods in Natural Language Processing: System Demonstrations*, pages 543–553, 2023. 1

[56] Zhu Zhang, Zhou Zhao, Yang Zhao, Qi Wang, Huasheng Liu, and Lianli Gao. Where does it exist: Spatio-temporal video grounding for multi-form sentences. In *Proceedings of the IEEE/CVF Conference on Computer Vision and Pattern Recognition*, pages 10668–10677, 2020. 5

[57] Hang Zhao, Antonio Torralba, Lorenzo Torresani, and Zhicheng Yan. Hacs: Human action clips and segments dataset for recognition and temporal localization. *Proceedings of the IEEE/CVF International Conference on Computer Vision*, pages 8668–8678, 2019. 3, 5

[58] Rongkun Zheng, Lu Qi, Xi Chen, Yi Wang, Kun Wang, Yu Qiao, and Hengshuang Zhao. Villa: Video reasoning segmentation with large language model. *arXiv preprint arXiv:2407.14500*, 2024. 1

Long-RVOS: A Comprehensive Benchmark for Long-term Referring Video Object Segmentation

Supplementary Material

Table 7. Definitions of the video attributes.

Attribute	Full Name	Definition
POC	Partial Occlusion	The target object is partially occluded in the sequence.
FOC	Full Occlusion	The target object is fully occluded in the sequence.
OV	Out-of-view	The target leaves the video frame completely.
LRA	Long-term Reappearance	Target object reappears after disappearing for at least 100 frames.
VC	View Change	Viewpoint affects target appearance significantly.
ARC	Aspect Ratio Change	The ratio of bounding box aspect ratio is outside the range [0.5, 2].
SV	Scale Variation	The ratio of any pair of bounding-box is outside of range [0.5,2.0].
CM	Camera Motion	Abrupt motion of the camera.
MB	Motion Blur	The boundary of target object is blurred because of camera or object fast motion.

Table 8. The percentage (%) of videos featuring specific attributes.

Dataset	POC	FOC	OV	LRA	VC	ARC	SV	CM	MB
MeViS [9]	54.8	15.1	28.7	0.1	10.0	88.2	78.7	49.2	18.8
Long-RVOS (Ours)	**60.5**	**36.2**	**61.0**	**11.5**	**25.9**	**96.2**	**93.6**	**60.7**	**28.7**

7. More Dataset Statistics

To further highlight the challenges posed by Long-RVOS, we present a statistical analysis of video attributes, with definitions provided in Table 7. As shown in Table 8, compared to the current largest dataset MeViS [9], Long-RVOS involves numerous long-video challenges, including frequent object occlusion (POC, FOC, and OV) and long-term object disappearance-reappearance (LRA). In addition, the videos in Long-RVOS exhibit significant object motion (CM and MB) and appearance changes (VC, ARC and SV), making the dataset more akin to real-world scenarios.

8. More Implementation Details

Motion Extraction. Following Video-LaVIT [20], we rely on motion vectors instead of the expensive dense optical flow. Formally, given a video clip, we partition each frame into 16 × 16 non-overlapping macroblocks. Then, motion vectors $\vec{m}$ of the t-th frame are estimated by matching the macroblocks between the adjacent frames I_t and I_{t-1}:

$$\vec{m}(p,q) = \arg\min_{i,j} \|I_t(p,q) - I_{t-1}(p-i,q-j)\|, \quad (6)$$

where $I(p,q)$ denotes the pixel values of the macroblock at location (p,q), and (i,j) denotes the coordinate offset between the centers of the two macroblocks. Empirically, the extraction of motion vectors runs at 748 FPS on our device (Intel(R) Xeon(R) Gold 6226R CPU @ 2.90GHz), enabling real-time processing of long videos.

Global Interaction. This module performs temporal attention over the inter-frame object features, enabling temporal reasoning and understanding. Since this is a common module in RVOS approaches [9, 27, 32], we follow the object-consistent temporal enhancer (OTE) of ReferDINO [27] rather than designing a new one from scratch. For clarity, we briefly revist OTE here. Given T-frame object features $\{O_t\}_{t=1}^{T}$ where $O_t \in \mathbb{R}^{N_q \times d}$, OTE utilizes the Hungarian algorithm [24] to align the N_q objects between adjacent frames based on the pairwise cosine similarity. After that, it performs temporal self-attention over the aligned object features and cross-attention with the sentence features $\widetilde{E}$. We refer the readers to the original paper [27] for additional details.

Training. Unlike previous RVOS methods, ReferMo relies only on the keyframe ground-truth annotations for efficient training. Formally, given a text description and a video of T_c clips, ReferMo outputs the prediction sequences $\{\mathbf{p}_i\}_{i=1}^{N_q}$ for the N_q object queries, where each sequence $\boldsymbol{p}_i = \{\hat{\boldsymbol{s}}_i^t, \hat{\boldsymbol{b}}_i^t, \hat{\boldsymbol{m}}_i^t\}_{t=1}^{T_c}$ describes the binary classification probability, bounding box and mask of the i-th object query on t-th keyframe. Our training pipeline follows the practice in previous approaches [27, 32, 48]. Suppose $\boldsymbol{y} = \{\boldsymbol{s}^t, \boldsymbol{b}^t, \boldsymbol{m}^t\}_{t=1}^{T_c}$ as the ground truth of keyframes, we select the prediction sequence with the lowest matching cost as the positive and assign the remaining sequences as negative. The matching cost is defined as follows:

$$\begin{aligned}\mathcal{L}_{\text{total}}(\boldsymbol{y}, \boldsymbol{p}_i) =& \lambda_{\text{cls}}\mathcal{L}_{\text{cls}}(\boldsymbol{y}, \boldsymbol{p}_i) + \lambda_{\text{box}}\mathcal{L}_{\text{box}}(\boldsymbol{y}, \boldsymbol{p}_i) \\ &+ \lambda_{\text{mask}}\mathcal{L}_{\text{mask}}(\boldsymbol{y}, \boldsymbol{p}_i).\end{aligned} \quad (7)$$

Table 9. Comparison on Long-RVOS valid set. FPS is estimated at 360P on Nvidia A6000 GPUs, excluding the video loading time.

Method	Static			Dynamic			Hybrid			Overall			FPS
	$\mathcal{J}$&$\mathcal{F}$	tIoU	vIoU	$\mathcal{J}$&$\mathcal{F}$	tIoU	vIoU	$\mathcal{J}$&$\mathcal{F}$	tIoU	vIoU	$\mathcal{J}$&$\mathcal{F}$	tIoU	vIoU	
Without SAM / SAM2													
SOC [32] NeurIPS'23	38.7	73.1	34.9	37.8	74.6	34.1	37.8	74.3	34.5	38.1	74.0	34.5	53.8
MUTR [52] AAAI'24	44.1	73.5	40.3	42.0	75.2	38.9	43.5	74.6	40.2	43.2	74.4	39.8	20.4
ReferDINO [27] ICCV'25	52.5	**74.2**	48.2	46.7	**75.2**	42.9	49.3	**74.8**	45.4	49.6	**74.7**	45.6	46.4
With SAM / SAM2													
VideoLISA [1] NeurIPS'24	17.3	66.8	12.7	12.9	72.6	6.8	12.1	72.3	6.0	14.1	70.5	8.6	6.6
GLUS [28] CVPR'25	24.4	62.8	20.8	26.1	64.7	23.1	24.1	63.5	20.6	24.8	63.7	21.5	3.6
SAMWISE [7] CVPR'25	42.3	61.5	31.2	40.7	63.3	31.4	40.6	65.8	31.2	41.2	63.5	31.2	7.0
RGA3 [45] ICCV'25	21.1	61.0	15.4	22.3	62.8	17.5	21.1	61.8	16.4	21.5	61.8	16.4	8.7
ReferMo (Ours)	**56.7**	74.0	**49.4**	**50.7**	74.2	**43.4**	**53.7**	74.7	**47.4**	**53.7**	74.3	**46.8**	52.5

The matching cost is computed on individual frames and normalized by T_c. Here, $\mathcal{L}_{\text{cls}}$ is the focal loss that supervises the binary classification prediction. $\mathcal{L}_{\text{box}}$ sums up the L1 loss and GIoU loss. $\mathcal{L}_{\text{mask}}$ is the combination of DICE loss, binary mask focal loss and projection loss [44]. λ_{cls}, λ_{box} and λ_{mask} are scalar weights of individual losses. The model is optimized end-to-end by minimizing the total loss $\mathcal{L}_{\text{total}}$ for positive sequences and only the classification loss $\mathcal{L}_{\text{cls}}$ for negative sequences.

Inference. ReferMo produces instance mask for the referring object on keyframes and then employs SAM2 [37] for subsequent frames. Specifically, for the prediction sequences $\{\mathbf{p}_i\}_{i=1}^{N_q}$, we select the best sequence with the highest average classification score as follows:

$$\sigma = \underset{i\in[1,N_q]}{\arg\max} \frac{1}{T_c} \sum\nolimits_{t=1}^{T_c} \hat{\boldsymbol{s}}_i^t \tag{8}$$

Then, the output mask sequence on keyframes is formed as $\{\boldsymbol{m}_\sigma^t\}_{t=1}^{T_c}$. For the t-th video clip, we use the keyframe prediction $\boldsymbol{m}_\sigma^t$ as the mask prompt for SAM2, which tracks the target across the subsequent frames within the clip.

9. Validation Results

In Table 9, we present the benchmark results on Long-RVOS validation set. The results show that our ReferMo achieves consistent improvements over previous RVOS methods, especially those built on SAM or SAM2.

10. More Ablation Studies

Effectiveness of Gating Image-Motion Fusion. ReferMo employs the spatial-aware gating (SG) and channel-aware gating (CG) mechanisms in image-motion fusion to avoid undesired motion noise. As shown in Table 10, directly concatenating keyframe and motion features leads to a performance collapse. This is because RVOS requires per-frame fine-grain perception, while directly integrating motion features can introduce significant object-irrelevant noise. By applying these two gating strategies, ReferMo effectively alleviates such noise while preserving only the motion cues that highlight target objects, thereby yielding significant performance gains.

Table 10. Keyframe results of different image-motion fusion approaches.

SG	CG	$\mathcal{J}$	$\mathcal{F}$	$\mathcal{J}$&$\mathcal{F}$
		28.8	28.7	28.7
✓		46.9	46.3	46.6
	✓	49.5	50.4	50.0
✓	✓	50.3	51.8	51.1

Table 11. Overall $\mathcal{J}$&$\mathcal{F}$ results for different description lengths.

Method	**<10**	**[10, 20]**	**>20**
RGA3 [45]	23.8	22.6	19.8
MUTR [52]	42.5	43.1	38.2
SAMWISE [7]	40.1	41.5	40.8
ReferDINO [27]	49.2	49.2	44.3
ReferMo (ours)	**53.6**	**53.6**	**48.5**

Table 12. Overall $\mathcal{J}$&$\mathcal{F}$ results by event complexity.

Method	***Single-event***	***Two-event***	***Multi-event***
RGA3 [45]	23.0	22.6	19.2
MUTR [52]	42.7	40.0	36.0
SAMWISE [7]	40.6	41.7	38.0
ReferDINO [27]	48.4	44.7	37.2
ReferMo (ours)	**52.9**	**48.0**	**40.5**

Effect of Description Length. We evaluate the impact of varying description lengths and present the results in Table R1. As description length increases, slight performance declines are observed across models. However, our ReferMo consistently outperforms existing methods across different description lengths.

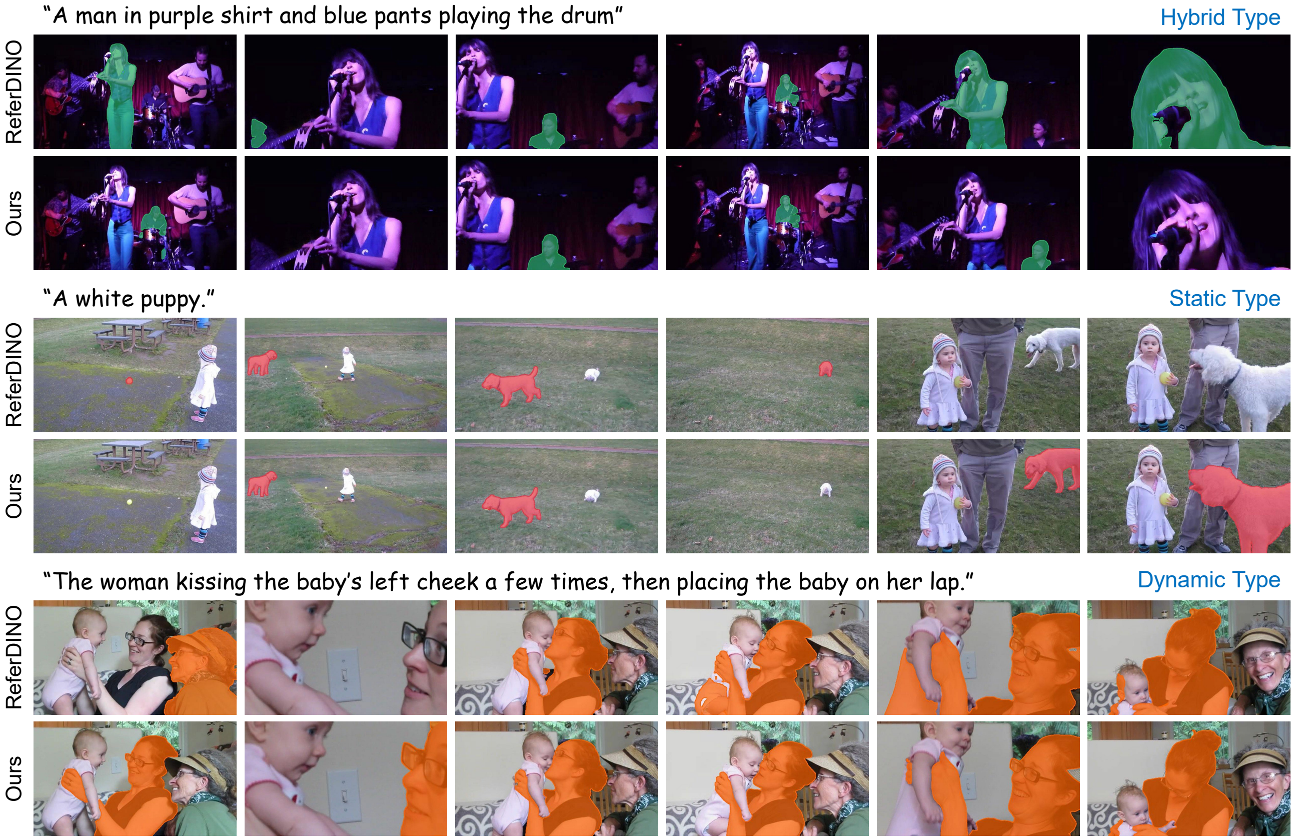
"A man in purple shirt and blue pants playing the drum"
Hybrid Type
ReferDINO
Ours
"A white puppy."
Static Type
ReferDINO
Ours
"The woman kissing the baby's left cheek a few times, then placing the baby on her lap."
Dynamic Type
ReferDINO
Ours

Figure 8. Qualitative comparison of our ReferMo with the SOTA model ReferDINO [27]. ReferMo performs better in long-term object consistency and segmentation quality.

Effect of Multi-event Videos. To explore the impact of event number in a video on model performance, we categorized the samples into single-event, two-event, and multi-event groups based on the keywords (e.g., *then*, *finally*, *ultimately*) in descriptions. As shown in Table 12, performance across models declines as the event number increases, yet our ReferMo consistently outperforms existing methods. Also, these results highlight the significance of our long-term benchmark for evaluating the capabilities of RVOS models in understanding complex event sequences.

11. Visualization

In Figure 8, we provide the qualitative comparisons with the SOTA model ReferDINO [27] on Long-RVOS. These examples involve multiple long-term challenges, such as object occlusion, disappearance-reappearance and view changes. The results clearly show the effectiveness of our baseline ReferMo in long-term object consistency and segmentation quality.

12. Limitations and Future Work

In this work, we chose to begin with description-based RVOS because it is commonly used in current video applications and this task remains far from being solved. It is promising to broaden the benchmark scope to support more tasks, such as reasoning RVOS [1, 51], semi-supervised VOS [10, 36, 50], interactive VOS [23, 37] and audio-guided VOS [52]. Besides, while our benchmark covers a variety of objects, it currently does not include background stuff classes (e.g., sky and river), which could be incorporated in future work for covering more diverse scenarios.